Taylor & Francis
Taylor & Francis Group

RESEARCH PAPER

🔓 OPEN ACCESS

Cellular mRNA recruits the ribosome via eIF3-PABP bridge to initiate internal translation

Nehal Thakor[a,c,*], M. Duane Smith[d], Luc Roberts[c], Mame Daro Faye[a,**], Harshil Patel[c], Hans-Joachim Wieden[c], Jamie H. D. Cate[d], and Martin Holcik[a,b]

[a]Apoptosis Research Center, Children's Hospital of Eastern Ontario Research Institute, Ottawa, Ontario, Canada; [b]Department of Pediatrics, University of Ottawa, Ottawa, Ontario, Canada; [c]Department of Chemistry and Biochemistry, Alberta RNA Research and Training Institute, University of Lethbridge, Lethbridge, AB, Canada; [d]Department of Molecular and Cell Biology, University of California, Berkeley, CA, USA

ABSTRACT

IRES-mediated translation of key cell fate regulating genes has been implicated in tumorigenesis. Concerted action of canonical eukaryotic initiation factors and IRES transacting factors (ITAFs) was shown to regulate cellular IRES mediated translation; however, the precise molecular mechanism of ribosome recruitment to cellular IRESes remains unclear. Here we show that the X-linked inhibitor of apoptosis (XIAP) IRES operates in an evolutionary conserved viral like mode and the structural integrity, particularly in the vicinity of AUG, is critical for ribosome recruitment. The binding of eIF3 together with PABP potentiates ribosome recruitment to the IRES. Our data support the model in which eIF3 binds directly to the XIAP IRES RNA in a structure-dependent manner and acts as a scaffold for IRES RNA, PABP and the 40S ribosome.

Introduction

Regulation of protein synthesis is a key cellular process which is intimately linked to cellular survival. Cells' ability to regulate translation is frequently focused on 2 key control points which are shared by virtually all mRNAs – components of the eIF4F complex and eIF2α. These regulatory points are utilized under normal growth conditions to match the protein output to the cell's growth, but also under physiological and pathophysiological conditions, which require adaptive changes in gene expression. Of particular interest is selective mode of translation initiation, which allows complete or partial bypass of the translation control points and is therefore essential for the reprograming of the cellular proteome under stress.[1,2] Selective translation is therefore a key mechanism which is required for cellular survival under stress and is used by cells to fine-tune their stress response.[3-5]

One example of selective translation is internal ribosome entry. This phenomenon, termed internal initiation, was first observed with RNA viruses (in particular *picornaviridae*) whose RNA is naturally uncapped and yet efficiently translated by the host translation machinery.[6] Instead of a cap, distinct functional RNA elements, termed IRES (Internal Ribosome Entry Site), precede the protein-coding portion of viral RNA and directly recruit the 40S ribosome to the vicinity of initiation codon. This recruitment can occur in the absence of any other protein factors (as with dicistrovirus intergenic IRES) or with the aid of various combinations of canonical initiation factors (such as eIF4G, eIF3, eIF5, and eIF5B) and auxiliary proteins in case of the remaining viral IRES. (reviewed in [7]) A small number of cellular mRNAs, in particular those encoding proteins that are key regulators of cell proliferation and survival/apoptosis, were suggested to be translated by this alternative mode of translation. However, and unlike viral IRESes, the molecular mechanism of ribosome recruitment and translation initiation on cellular IRES is virtually unknown.

Given this gap we wished to determine how the ribosome is recruited to a cellular IRES. We used an IRES from an inhibitor of apoptosis, XIAP, which has been extensively characterized for its sequence, structure, and auxiliary factor requirements.[8-14] We have used a previously established *in vitro* toeprinting system that faithfully recapitulates formation of the initiation complex on an uncapped XIAP IRES[15] and found that XIAP IRES uses a virus-like mode of ribosome recruitment in which the eukaryotic initiation factor 3 (eIF3) is recruited directly to the precise structural conformation near the initiating AUG in a poly(A)- and PABP-dependent manner. The canonical initiation factors of the eIF4F complex are not required for the XIAP IRES initiation, thus explaining why XIAP expression is not attenuated during cellular stress.

Results

Conformation of the XIAP IRES is critical for initiation complex formation

Translation initiation on XIAP IRES relies on eIF5B when global protein translation is attenuated due to eIF2α

phosphorylation.[15] Using the toeprinting assay we have extensively characterized uncapped XIAP IRES RNA for initiation complex formation in RRL and showed that it can only be formed on either the 5′ cap-containing, or IRES-containing RNAs (Fig. S1A).[15] Furthermore, XIAP IRES forms initiation complex on the authentic initiation codon AUG[15] since mutating this codon (SC mutant; AUG to AAG) blocked formation of the initiation complex (Fig. S1B). Interestingly, 2 point mutations in the polypyrimidine tract (PPT) of the XIAP IRES abolished the ability of the IRES to form initiation complex.[15] We further wished to determine the underlying mechanism of initiation complex formation on the XIAP IRES. We hypothesized that conformation of the IRES is significantly altered by the PPT mutations resulting in an inability of this IRES mutant to support initiation complex formation. In order to verify this hypothesis, we generated additional mutants of the XIAP IRES and determined their ability to form initiation complex in GMP-PNP and ATP treated RRL. We observed that neither the 5′ PPT mutant ($_{-43}$UU$_{-44}$ to $_{-43}$AA$_{-44}$; [15]) nor the 3′ PPT mutant ($_{-1}$AA$_{-2}$ to $_{-1}$UU$_{-2}$) could form initiation complex when used as uncapped RNA (Fig. 1B). However, these mutants were able to form initiation complex when 5′ cap was incorporated suggesting that they were impaired in the ribosome recruitment step. The double PPT mutant harboring both $_{-43}$UU$_{-44}$ to $_{-43}$AA$_{-44}$ and $_{-1}$AA$_{-2}$ to $_{-1}$UU$_{-2}$ mutations was able to form initiation complex without the need for 5′ cap (Fig. 1B). These mutant versions of the XIAP IRES were generated based on the previously published XIAP UTR secondary structure.[9] Of the note, there is an error (point mutation; $_{-8}$A to $_{-8}$C) in the previously published sequence/RNA secondary structure (RSS), which was introduced by erroneously using mouse XIAP sequence as a template for the primer to generate the IRES construct. Additionally, the previous RSS[9] of the XIAP IRES did not include XIAP coding sequence (CDS), whereas, the XIAP IRES construct used in this study contains 42 NT of XIAP CDS.[15] Therefore, we anticipated that this XIAP IRES RNA fragment would fold significantly different from the previously determined RSS of the XIAP IRES.[9] Accordingly, all IRES variants were subjected to selective 2′-hydroxyl acylation analyzed by primer extension (SHAPE) analysis (Fig. S6). Furthermore, using the NMIA reactive sites (Table S3; lowercase NTs in Figs. 1A, 2A, 4A and S3A) of the RNA sequences, in RNASTRUCTURE program,[20] we have generated RSS models for all the variants of the XIAP IRES (Fig. 1A). Of note, for both 5′ PPT and 3′ PPT mutations individually, the NMIA reactive sites were significantly altered (Fig. S6 & Table S3) when compared to XIAP IRES RNA and the RSS were distorted (Fig. 1B). However, combination of both mutations restored the secondary structure of XIAP IRES RNA (Fig. 1B) and the NMIA reactive sites were comparable to that of the XIAP IRES RNA (Fig. S6 and Table S3). These data strongly suggest that the conformation of the XIAP IRES RNA is critical for the formation of initiation complex. In concordance with this model, the NMIA reactive sites of the alternatively spliced 5′ UTR of XIAP (non-IRES UTR), which does not confer IRES activity[25] or initiation complex formation (Fig. S3), is significantly different from the XIAP IRES

(Fig. S6G & Table S3) and it folds into a significantly different conformation from the XIAP IRES UTR.

XIAP coding sequence takes part in ribosome recruitment and the local conformation of RNA in the vicinity of AUG is critical for initiation complex formation

Having established the importance of proper secondary structure of the XIAP IRES for initiation complex formation we wanted to define the minimal region of the XIAP IRES that is required for ribosome recruitment. We generated progressive deletions of the XIAP IRES (Fig. 2A) and determined their ability to form initiation complex. The ability of truncated versions of the XIAP IRES (−103, −83, −61, −49, −44, −38 and −33) to form initiation complex remained unaffected (Fig. 2B). Further truncations (−14, +1 & +4) significantly decreased the ability to form initiation complex. Removal of AUG (truncation +4) completely abolished initiation complex formation in accordance with our previous observation.[15] Additionally, mutating the initiation codon AUG to AAG in either the full length or truncated (−33) variant of the IRES resulted in the loss of initiation complex formation (Fig. S1B). As these observations suggest that only 33 NT upstream of AUG are sufficient to form initiation complex, they prompted us to investigate the putative role of the XIAP coding region in ribosome recruitment and initiation complex formation. We thus generated 2 RNA chimeras (Fig. 3A), which contained either 33 nucleotides of XIAP 5′ UTR and 42 nucleotides of GAPDH coding region (RNA chimera A), or 33 nucleotides of GAPDH 5′ UTR and 42 nucleotides of XIAP coding region (RNA chimera B), and tested their ability to support initiation complex formation. Unexpectedly, RNA chimera A did not form initiation complex while the RNA chimera B did (Fig. 3A). In order to test the translational competence of chimera B we performed additional toeprinting assay in GMP-PNP or GTP treated RRL and determined the distribution of fluorescence intensity of the leading edge toeprints as described.[15,26] The fluorescence intensity distribution of either variant of the XIAP IRES (17≥18>19) was consistent with the formation of 48S initiation complex (Fig. 3B, left and middle panel). Furthermore, in GTP-treated RRL the fluorescence intensity distribution shifted (17<18>19) which is indicative of 80S initiation complex formation.[15-26] In contrast, the RNA chimera B remained insensitive to GTP treatment and formed 48S initiation complex (fluorescence intensity 17<18>19) both in GMP-PNP and GTP treated RRL. This suggests that while the sequences within the XIAP coding region are needed for the formation of the initiation complex, this complex is not translation competent.

These observations raised a concern about the reliability of using published XIAP IRES bicistronic reporter construct, in which the XIAP coding region is replaced with that of chloramphenicol acetyl transferase (CAT) gene.[27] In order to address this concern, we generated an RNA chimera in which the XIAP coding region was replaced with that of CAT (−33 CAT version), and used it to perform toeprinting assay in RRL. In contrast to the −33 version of XIAP IRES (Fig. 2), the uncapped −33 CAT RNA chimera did not form initiation complex,
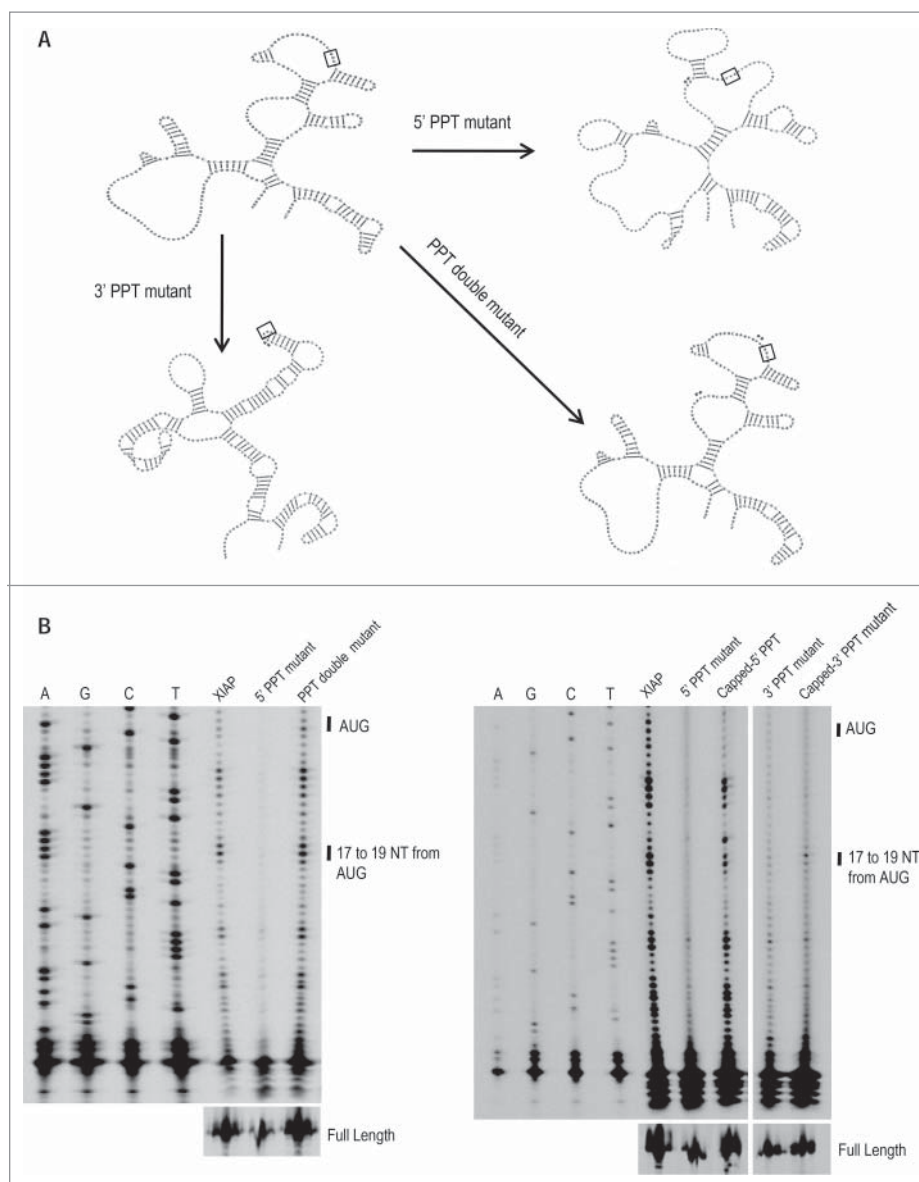
Figure 1. Conformation of XIAP IRES RNA is critical for initiation complex formation. (A) Schematic diagram of RNA conformation of XIAP IRES RNA and its mutated versions as revealed by N-methylisotoic anhydride (NMIA) probing. Initiation AUG codon is boxed; mutated bases are indicated by asterisks. (B) Capped and un-capped versions of wildtype and mutated XIAP IRES RNA (5′ PPT mutant (panel A) in which the indicated UU was mutated to AA; 3′ PPT mutant (panel A) in which the indicated AA was mutated to UU; PPT double mutant (panel A) in which the indicated UU was mutated to AA and the indicated AA was mutated to UU) were subjected to toeprinting analysis in RRL. While the individual PPT mutations abolished the ability of XIAP IRES to form initiation complex the double mutant that restores XIAP IRES RNA conformation was able to form initiation complex.

whereas the capped version of −33 CAT RNA chimera did (Fig. S2A). However, CAT. RNA chimera containing longer (170 NT) XIAP IRES, which mimics the sequence composition of the bicistronic mRNA, formed initiation complex in RRL without the requirement for 5′ cap (Fig. S2B). These data suggest that the full length XIAP IRES UTR makes the RNA conformation permissive for ribosome recruitment and initiation complex formation (in a toeprinting assay) possibly by affecting the local RNA conformation in the vicinity of AUG. Furthermore, inclusion of 42 NT XIAP CDS in the bi-cistronic reporter construct (upstream of CAT CDS) had no significant effect on the XIAP IRES activity (Fig. S2C). Of note, XIAP IRES deletions in the context of the bicistronic construct further support this possibility since the truncations extending past the 100 nucleotides of the 5′ UTR impaired the IRES activity.[8,12]

Furthermore, RNAs consisting of the XIAP non-IRES UTR with 42 nucleotides of XIAP coding region (Fig. S3), or the 5′ and 3′ PPT mutants (Fig. 1), which fold differently from XIAP IRES (in particular in the vicinity of AUG) did not support initiation complex formation. This evidence, collectively with the XIAP-CAT RNA chimera data suggest that local conformation of the RNA in the vicinity of AUG determines the ability of RNA to recruit ribosome and to form translationally competent initiation complex.

In order to validate this model, we first obtained the NMIA reactive sites (Fig. S6E & Table S3) and modeled RSS −33 XIAP IRES RNA (Fig. 4A) using RNASTRUC-TURE program.[20] Subsequently, we mutated $_{40}CC_{41}$ to $_{40}GG_{41}$ to generate −33 XIAP IRES RNA CDS mutant with altered RNA conformation in the vicinity of AUG, as
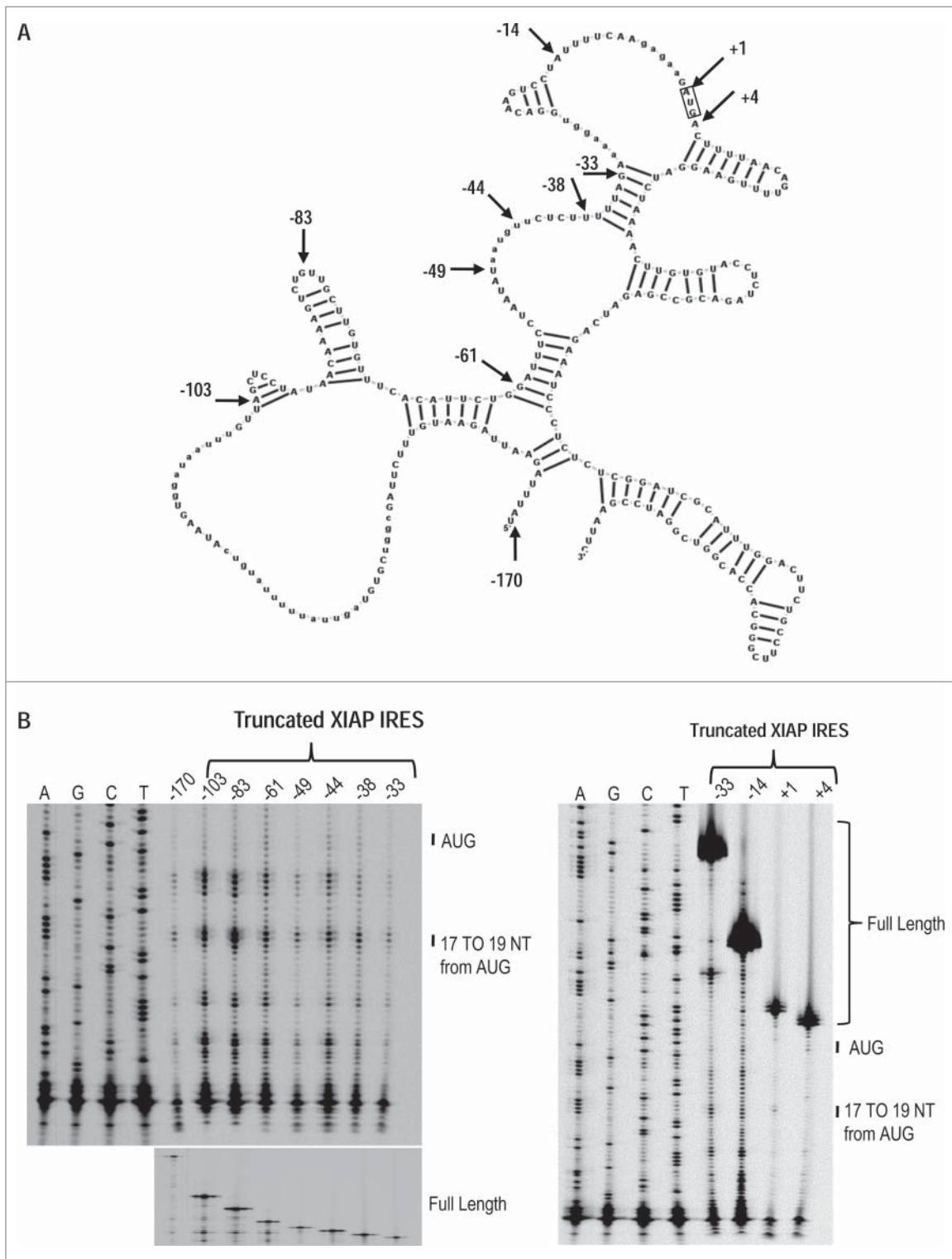
Figure 2. Determination of minimal ribosome recruiting cis-element of XIAP IRES RNA. (A) Schematic of truncated versions of XIAP 5′ UTR that were generated to map the ribosome recruitment site on XIAP RNA. Arrows and numbers indicate positions of truncations. Initiation AUG codon is boxed. (B) Truncated versions of XIAP 5′ UTR were subjected to toeprinting assay in GMP-PNP treated RRL. Ability of XIAP IRES RNA to form initiation complex was not affected significantly when 67, 87, 109, 121, 126, 132 and 137 NT were truncated starting from 5′ end (−170, −103, −83, −61, −49, −44, −38 and −33 respectively). However, larger truncations of 156 and 170 NT (−14 and +1 respectively) lead to the decreased ability of XIAP IRES to form initiation complex.

confirmed by the NMIA reactive sites and RSS model (Fig. 4A, S6F & Table S3). Importantly, this mutant did not support initiation complex formation, in contrast to its parental variant (Fig. 4B). This observation strongly suggests that local RNA conformation in the vicinity of AUG

is critical and makes RNA either permissive or non-permissive for ribosome recruitment and initiation complex formation. This is similar to most viral IRESes which recruit ribosome within the 3′ border of the IRES (in the vicinity of AUG).[28] In addition, published data for viral IRESes
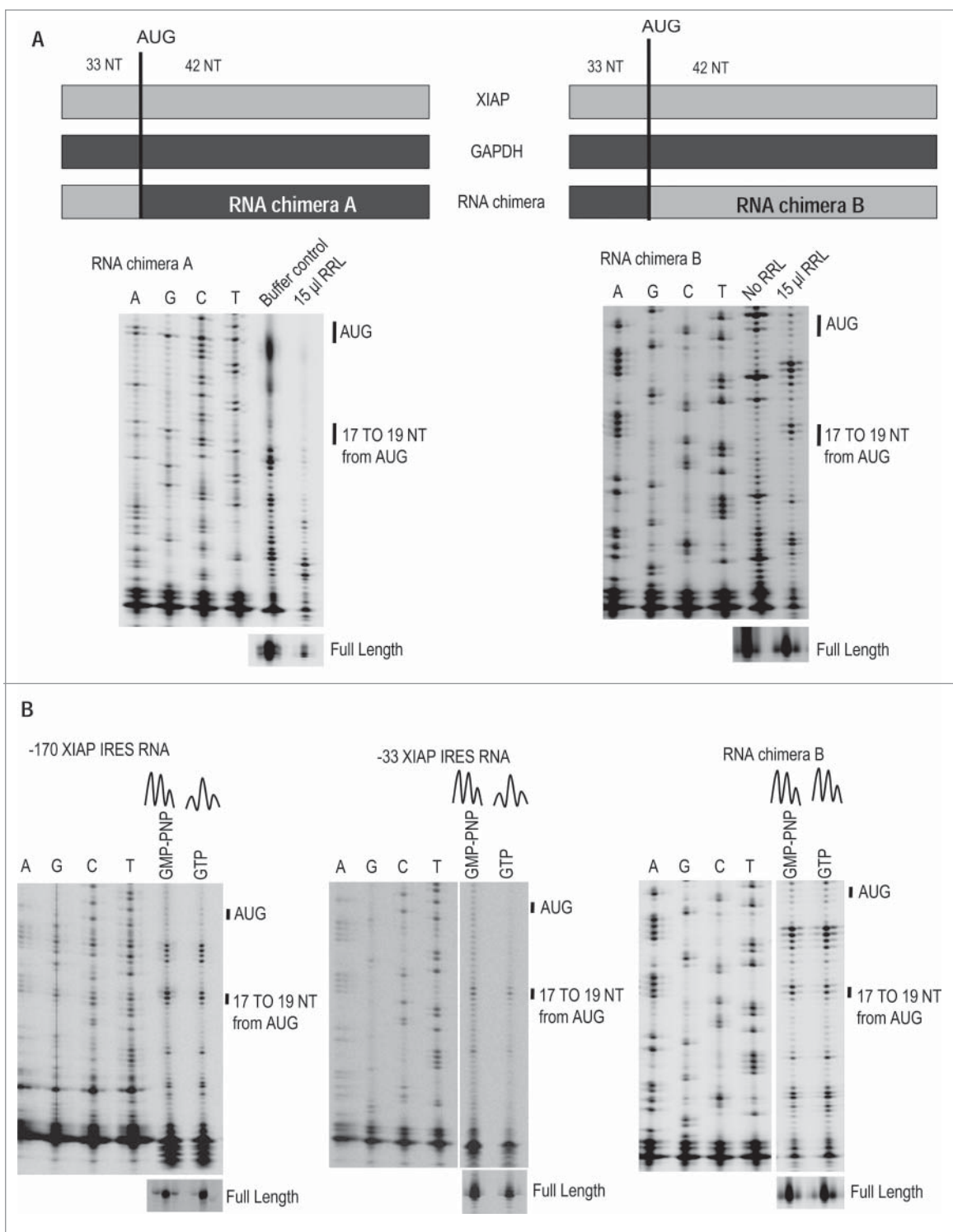
Figure 3. XIAP coding sequence takes part in ribosome recruitment, but the 3′ end of XIAP 5′ UTR (33NT) is required for translation competent initiation complex formation on AUG. (A) Schematic (top) of the RNA chimeras used in toeprinting assays (bottom). RNA chimera containing 33 NT of XIAP 5′ UTR and 42 NT of GAPDH coding sequence (RNA chimera A) was not able to form initiation complex. However, RNA chimera containing 33 NT of GAPDH 5′ UTR and 42 NT of XIAP coding sequence (RNA chimera B) formed initiation complex. (B) Toeprinting assays were performed in RRL pretreated with GMP-PNP or GTP. The distribution of fluorescence intensity of 40S leading edge toeprints are indicated on the top of each lane. 48S and 80S initiation complexes were differentiated as described (15,26). XIAP IRES RNA (−170; Fig. 2) (left panel) and its truncated version (−33; Fig. 2) (middle panel) were able to form 80S initiation complex in GTP treated RRL. However, RNA chimera B (right panel) did not form 80S initiation complex in GTP treated RRL.

clearly suggests that disruptions of RNA conformation around AUG adversely affect ribosome positioning and translation efficiency.[23,29,30] Here for the first time we show that, similar to viral IRES, cellular IRES also function in a RNA structure-dependent manner.

Ribosome is placed in the vicinity of AUG via poly(A) tail to form initiation complex on the IRES

Formation of the initiation complex on the XIAP IRES RNA requires polyA tail,[15] but the involvement of PABP or other
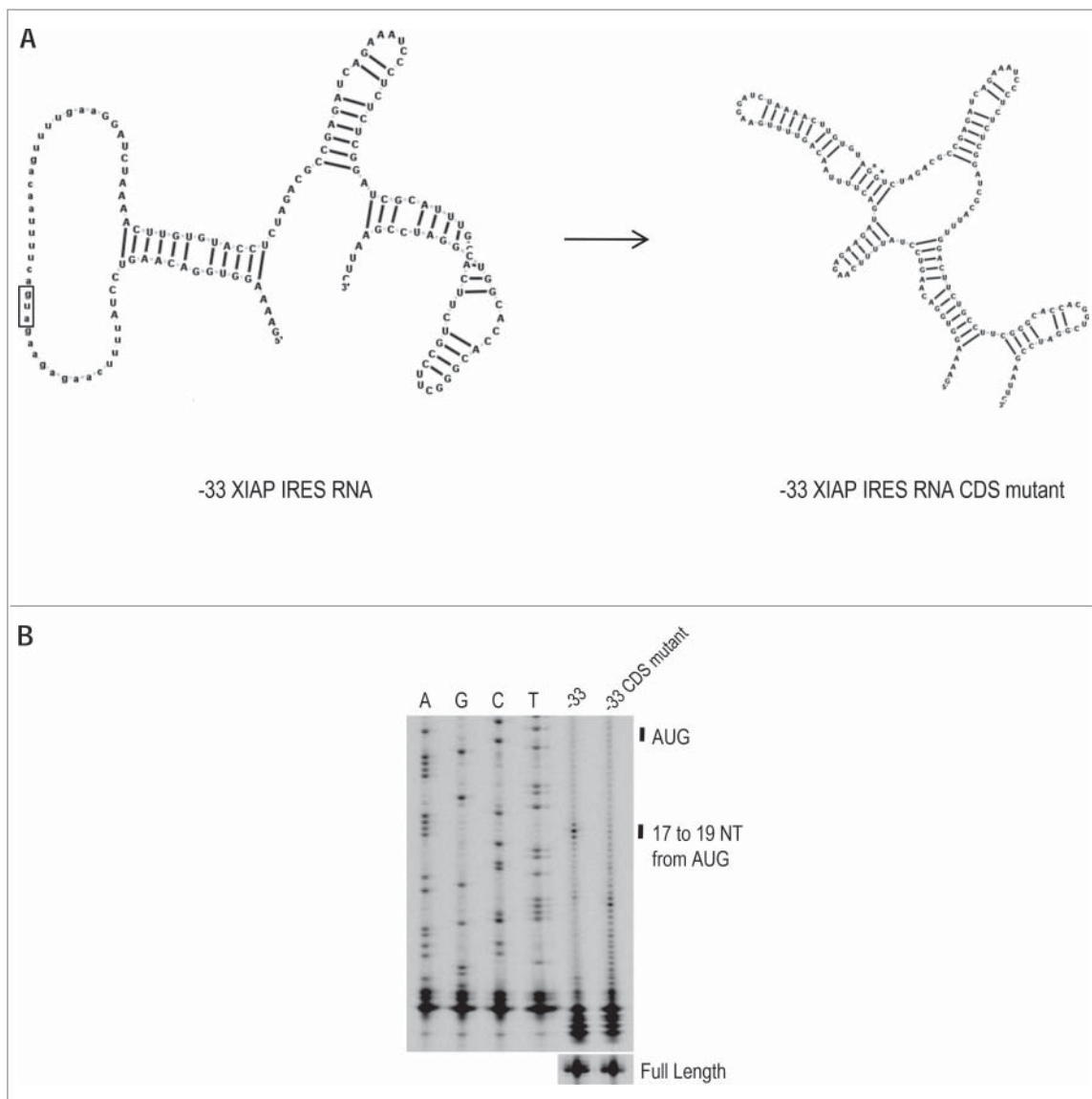
Figure 4. Conformation of minimal ribosome recruiting cis-element of XIAP IRES RNA is critical for initiation complex formation. (A) RNA conformation of −33 XIAP IRES RNA and its mutated versions as revealed by NMIA probing. Initiation AUG codon is boxed. Mutated bases (CC to GG) are indicated by asterisks. (B) WT and mutant versions of the −33 XIAP IRES RNA were subjected to toeprinting assay in RRL. Two point mutations in XIAP CDS which distorted RNA conformation of −33 XIAP IRES RNA also abolished its ability to form initiation complex formation.

eIFs in this process remains unknown. To address this requirement, first we performed toeprinting assays in RRL using XIAP IRES RNA with and without poly(A) tail. For comparison we performed toeprinting assays using Cricket Paralysis Virus (CrPV) IRES, which mimics tRNA structure and can initiate translation without the requirement for eIF4F and eIF2 by docking directly into the ribosome.[23] As expected, CrPV IRES RNA formed initiation complex in RRL in a poly(A) tail independent manner (Fig. 5A, right panel). In contrast, removal of the fifty-one thymidine residues poly(A) tail blocked initiation complex formation on the XIAP IRES RNA (Fig 5A, left panel). Similarly, Thoma et al.,[31] have reported that BiP and c-myc IRESes require poly(A) tail for translation initiation. However, these IRESes form initiation complex in a poly(A) binding protein 1 (PABP)-independent manner.[31] Accordingly, we sought to determine if PABP is needed for ribosome recruitment and initiation complex formation on the XIAP IRES we used

PABP-interacting protein 2 (PAIP2) to render PABP inactive, and performed toeprinting assay using both XIAP IRES RNA and CrPV IRES RNA. PAIP2 interacts directly with PABP and masks its poly(A) binding sites, and was shown to inhibit translation of poly(A) tailed RNAs in RRL by PABP sequestration.[21] XIAP IRES initiation complex formation was inhibited in GST-PAIP2 supplemented RRL but remained unaffected in GST treated RRL (Fig. 5B, left panel). In contrast, CrPV IRES initiation complex formation was resistant to GST-PAIP2 treatment (Fig. 5B, right panel). These data demonstrate that, unlike BiP and c-myc IRESes, both poly(A) tail and PABP are essential for the initiation complex formation on the XIAP IRES.

Typical eukaryotic mRNA contains 5′-end cap structure which facilitates translation initiation by binding to eIF4F complex (consisting of eIF4E, eIF4G and eIF4A). The helicase activity of eIF4A helps ribosome in scanning through the structured UTRs to locate authentic AUG.[32] We have previously shown
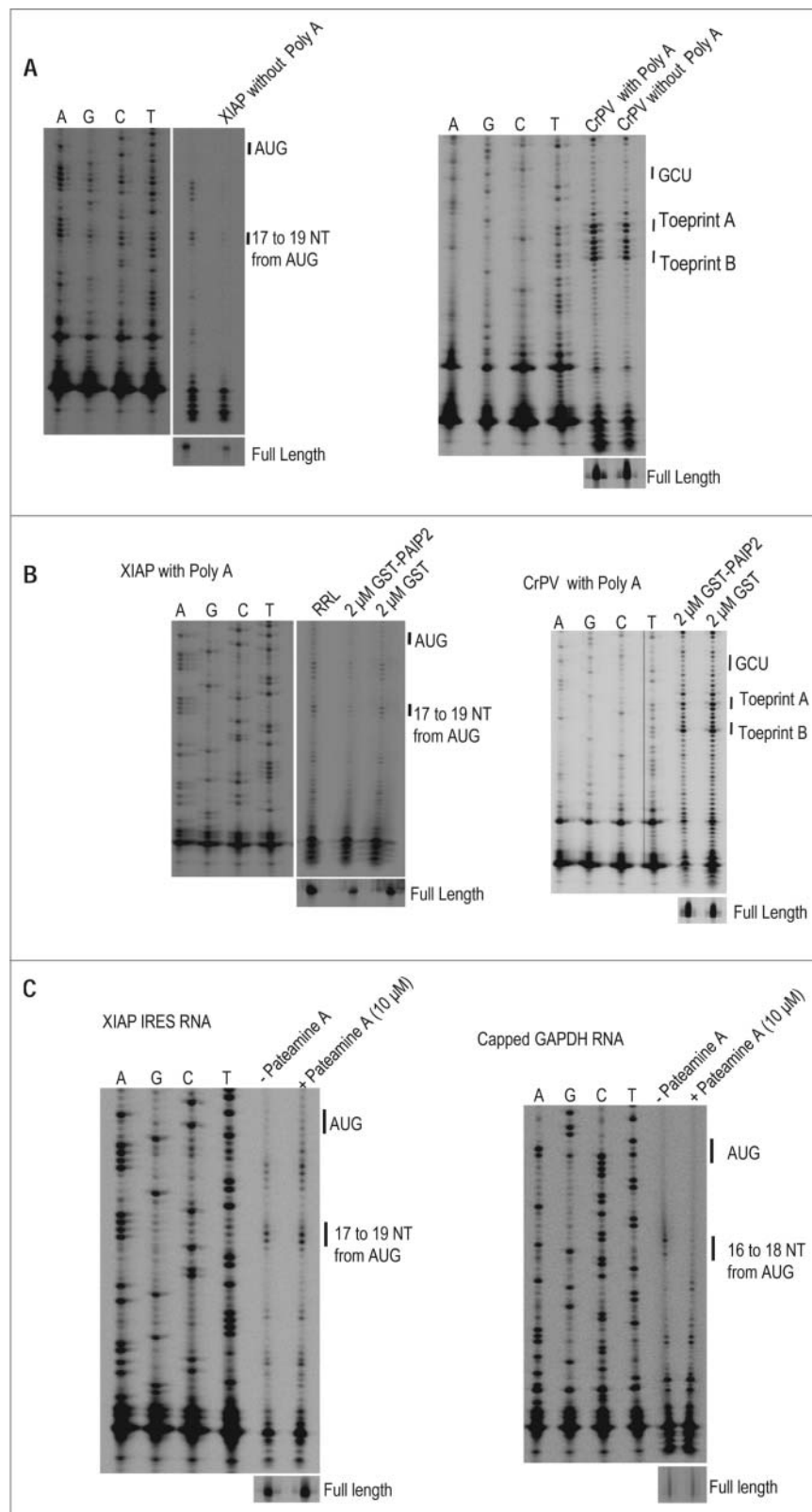
Figure 5. Poly(A) tail dependent initiation complex formation on XIAP IRES. (A) The ability of XIAP IRES RNA to form initiation complex was impaired in the absence of a poly(A) tail (left panel). However, the ability of CrPV IRES RNA, which mimics tRNA structure and directly binds to 40S ribosomal subunit, was unaffected in the absence of poly(A) tail (B) PAIP2, which destabilizes the interaction of PABP with poly(A) tail, impairs the ability of poly(A) tailed XIAP IRES RNA to form initiation complex. In contrast, the ability of CrPV IRES RNA to form initiation complex remained unaffected in PAIP2 supplemented RRL. (C) The activity of eIF4A is not required for XIAP IRES initiation complex formation. Initiation complex formation was inhibited by Pateamine A on capped non-IRES RNA (right panel). In contrast, XIAP IRES initiation complex formation remained unaffected in Pateamine A treated RRL (left panel).

that initiation complex formation on the XIAP IRES is not inhibited by hippuristanol, an eIF4A-specific ATPase inhibitor.[15] Pateamine A is a small chemical molecule which sequesters eIF4A and prevents it from participating in ribosome recruitment step. Treatment with Pateamine A inhibited cap-dependent translation initiation of GAPDH (Fig. 5C, right panel), while the XIAP IRES initiation complex formation remained unaffected (Fig. 5C, left panel). As hippuristanol and Pateamine A inhibit both eIF4A1 and eIF4A2, these data suggest that neither eIF4A1 nor eIF4A2 *per se*, nor their helicase activity are required for translation initiation on the XIAP IRES. Additionally, we have shown that only 33 NT upstream of AUG is sufficient to support formation of translation competent initiation complex on the XIAP IRES and that RNA conformation in the vicinity of AUG is critical for XIAP IRES initiation complex formation. Collectively, these data suggest that, like many viral IRESes, initiation complex formation on the XIAP IRES does not require eIF4A dependent ribosome scanning and the ribosome is likely positioned directly in the vicinity of AUG by a poly(A) tail- and PABP- dependent mechanism.

Ribosome recruitment on the XIAP IRES is directed by eIF3

During cap-dependent translation initiation, the circularization of 5′ capped mRNA, which is an early step of initiation, is mediated by interaction of poly(A) tail bound PABP and 5′ cap associated eIF4G.[32] This is a critical step of translation initiation which is thought to enhance both the efficiency of translation initiation as well as re-initiation (ribosome turn-over). There are numerous reports which suggest that eIF4G also supports cap-independent translation of both cellular and viral IRESes.[14,31,33-36] The strict dependence of XIAP IRES-mediated translation initiation on poly(A) tail and PABP prompted us to investigate if eIF4G is involved in initiation complex formation on the XIAP IRES as well. In addition, we wished to determine if any other ribosome associated eIFs interact with uncapped XIAP IRES RNA. To this end we performed XIAP IRES RNA affinity chromatography in S10 HeLa cell lysate as described.[15,18] As we expected PABP to bind to all RNA species, the levels of PABP were considered as a reference for protein loading. We observed that eIF2α, a subunit of ternary complex (eIF2-GTP-initiator tRNA), which normally binds to 43S ribosome was not present in the RNP complex formed on XIAP IRES RNA or its truncated version (Fig. 6A). Similarly, the eIF4E and eIF4A were also not part of the RNP complex assembled on the XIAP IRES RNA or its truncated version (Fig. 6A) which is in accordance with our hippuristanol and pateamine A data and the absence of cap on the bait RNA (Fig. 5C and[15]). In contrast, however, and contrary to our expectations we failed to detect eIF4G in the RNP complexes formed on XIAP IRES RNA (Fig. 6A). Additionally, immuno-inactivation of eIF4G did not alter the ability of XIAP IRES to form initiation complex in RRL (Fig. S4). Surprisingly, we detected eIF3d associated with XIAP IRES RNA and all its truncated versions (Fig. 6A). Of note, eIF3d also interacted with +1 and +4 truncated versions which contain only XIAP CDS but no UTR (Fig. 6A).

Two observations, namely the strong dependence of XIAP IRES initiation complex formation on PABP and the

presence of eIF3d in XIAP IRES RNP complex, prompted us to investigate if PABP and eIF3 work in synergy to form XIAP IRES initiation complex. To this end we performed RNA affinity chromatography in the presence or absence of poly(A) tail. In addition, we used the CrPV IRES RNA, with or without the polyA tail as a negative control. A general RNA binding protein YB-1 was used as a loading control.[37] As expected, we did not detect eIF4A, eIF4G or eIF4E in the RNP complex formed on either CrPV IRES or −33 XIAP IRES RNAs. Additionally, eIF3d interacted more profoundly with −33 XIAP IRES RNA than CrPV IRES RNA (Fig. 6B). As expected, more PABP bound to the poly (A)-tailed than to non-poly(A)-tailed RNAs. Importantly, the binding of eIF3d to −33 XIAP IRES RNA was significantly decreased in the absence of polyA tail. These data
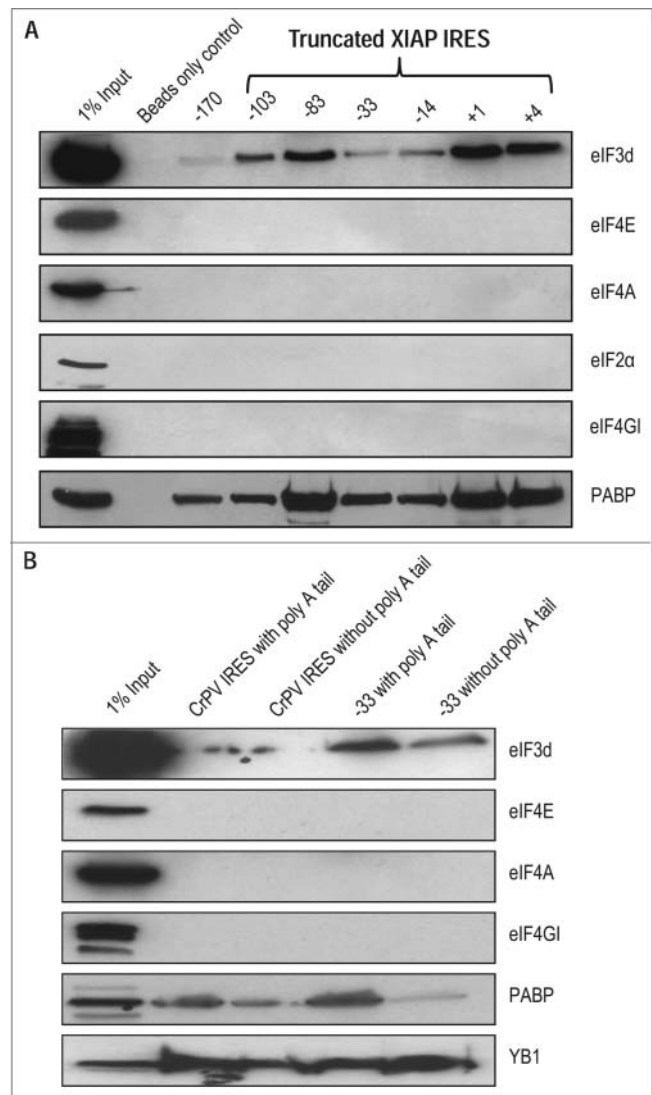

Figure 6. XIAP IRES RNA-associated initiation factors. (A) Streptomycin-RNA affinity chromatography was performed using uncapped truncated versions of XIAP IRES RNA as described (15). Effluents obtained from the streptomycin column were subjected to western blot analysis with indicated antibodies. (B) Streptomycin-RNA affinity chromatography was performed using poly(A) tailed and non-poly(A) tailed versions of XIAP IRES RNA and CrPV IRES RNA. Effluents obtained from the streptomycin column were subjected to protein gel blot analysis with indicated antibodies.

suggest that PABP enhances the recruitment of eIF3d to the XIAP IRES.

We further wished to determine if there is a direct interaction between eIF3 and XIAP IRES RNA. To this end we performed gel mobility shift assay in native condition using purified eIF3. ^{32}P labeled XIAP (wild type or PPT mutant) or CrPV IRES RNAs, were incubated with purified human eIF3 complex.[22] We observed that the mobility of eIF3-XIAP IRES RNA complex was retarded on the agarose gel suggesting that eIF3 (or its subunits) interacted directly with the XIAP IRES (Fig. 7A). eIF3 failed to retard mobility of the CrPV IRES (Fig. 7A). In contrast to XIAP IRES RNA, and in an agreement with our model, translationally incompetent XIAP IRES PPT mutant did not interact with eIF3 (Fig. 7A). These observations
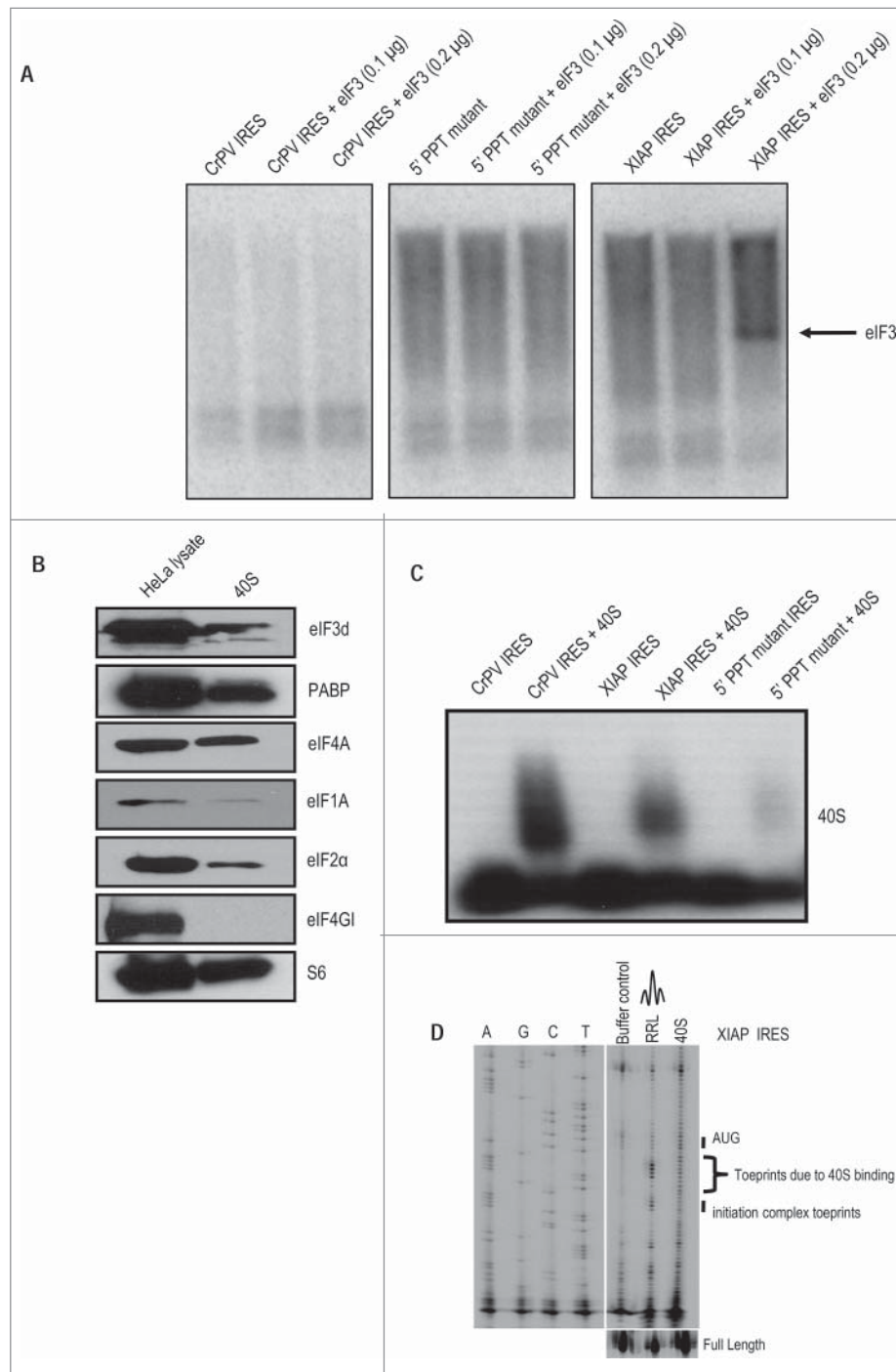

Figure 7. eIF3, the scaffolding protein, recruits ribosome on XIAP IRES RNA. (A) The ability of purified human eIF3 complex to bind XIAP IRES RNA was tested by electromobility shift assay in native conditions. eIF3 complex binds directly to the XIAP IRES RNA. In contrast, PPT mutant and CrPV IRES were unable to bind to eIF3 complex. (B) 40S ribosome subunits (salt non-washed) were purified, with its associated protein factors, from HeLa cells. Western blot analysis was performed to detect the presence of 40S associated proteins. (C) The ability of purified 40S ribosomal subunits was tested by electromobility shift assay. While the XIAP IRES RNA was able to bind to 40S subunit, the non-functional PPT mutant was unable to bind to 40S subunit. (D) The interaction between XIAP IRES RNA and 40S subunit was further characterized by toeprinting analysis.

suggest that eIF3, which normally interacts with 40S ribosome, likely bridges ribosome directly to XIAP IRES RNA in the vicinity of AUG without the need for eIF4F complex. In this case eIF3 acts as a scaffolding protein complex, instead of eIF4G, which together with PABP recruits ribosome to the 3′ border of XIAP IRES RNA.

We further wished to determine if the purified 40S ribosome, along with ribosome-associated initiation factors including eIF3, is recruited on the XIAP IRES. To this end we purified 40S ribosome complex from HeLa cells. As expected we did not find eIF4G associated with 40S ribosome complex while all other key eIFs (eIF3, eIF2, eIF4A, eIF1A and PABP) were present in the ribosome preparation (Fig. 7B). We performed ribosome binding assay using ^{32}P labeled CrPV IRES RNA, XIAP IRES RNA and XIAP PPT mutant RNA as described.[23,24] As previously published,[24] CrPV IRES RNA was bound by 40S ribosome complex and its mobility was retarded on the agarose gel (Fig. 7C). Similarly, the mobility of XIAP IRES RNA was decreased when incubated with 40S ribosome complex suggesting stable RNA-40S complex. However, the translationally incompetent PPT mutant failed to bind to 40S ribosome complex (Fig. 7C). To further characterize the nature of the ribosome-XIAP IRES interaction we used the toeprinting assay with either RRL or purified 40S. We observed formation of 80S initiation complex on XIAP IRES RNA in GTP and ATP treated RRL. In contrast, since the 40S ribosome preparation is void of the 60S ribosome subunit we did not clearly observe 80S initiation complex toeprints in 40S-XIAP IRES RNA toeprinting assay. However, we obtained several toeprints in the vicinity of AUG which are indicative of ribosome recruitment site on XIAP IRES RNA (Fig. 7D). These observations strongly suggest that eIF3 potentiates ribosome recruitment in the 3′ border of XIAP IRES RNA. Furthermore, eIF3 and PABP act together for ribosome recruitment and initiation complex formation on XIAP IRES RNA. These observations also suggest that translation initiation on XIAP IRES operates in virus-like mode. This notion is also supported by our previous report showing dependence of XIAP IRES on eIF5B during stress condition.[15]

Discussion

XIAP, a potent Inhibitor of Apoptosis protein, interacts with the effector caspases to inhibit apoptosis and provides a critical cell survival switch during physiological and pathophysiological stress conditions.[38] During such stress conditions expression of XIAP is translationally up-regulated *via* an IRES element thus providing survival advantage to cells.[8,13,39-43] We have previously shown that IRES mediated translation of XIAP relies on eIF5B during eIF2 phophorylation conditions.[15] However, the mechanism of ribosome recruitment on XIAP IRES during stress conditions remains unclear. In the present study we show that similar to some viral IRESes, XIAP IRES recruits ribosome directly to the vicinity of AUG and the local RNA conformation is crucial for this recruitment. Furthermore, eIF3, with PABP, acts as a scaffolding protein complex which directly interacts with the XIAP IRES RNA to recruit ribosome.

Viral IRESes are classified in 4 different groups based on their structural complexity and their requirement for canonical eIFs and trans-acting factors.[44] Structural similarity, despite the sequence dissimilarity within the groups of viral IRESes has been observed.[9] Mutational analyses have clearly shown that intrinsic secondary structure of viral IRESes is critical for ribosome recruitment.[23,24,45-49] The RNA secondary structures of several cellular IRESes have been determined by enzymatic or chemical probing,[9,50-54] but no structural similarity among cellular IRESes has been reported.[9] Additionally, mutational analysis of c-myc, Apaf-1 and Bag-1 IRESes has been reported and their ribosome landing cis-elements have been identified.[51,55,56] We have shown previously that 2 point mutations within the polypyrimidine tract of the XIAP IRES (5′ PPT mutant, $_{-43}UU_{-44}$ to $_{-43}AA_{-44}$) rendered it inactive.[8] Subsequently, using an *in vitro* toeprinting assay we have shown that the very same mutations rendered the XIAP IRES unable to form initiation complex in RRL ([15] and Fig. 1)). The 5′ PPT mutant or the 3′ PPT mutant ($_{-1}AA_{-2}$ to $_{-1}UU_{-2}$) alone distorted the intrinsic XIAP IRES conformation (Fig. 1B) likely due to a major change in the free nucleotide energy of RNA. This distortion of IRES structure resulted in the inability of the mutant RNAs to form initiation complex. However, when we combined 5′ PPT and 3′ PPT mutations, the RNA regained its intrinsic conformation and supported formation of the initiation complex in RRL (Fig. 1B). Of note, the alternatively spliced XIAP mRNA variant which does not harbor IRES element in the 5′ UTR folds significantly differently from the XIAP IRES UTR and is non-permissive for initiation complex formation in RRL in the absence of cap (Fig. S3). These data have clearly illustrated that the intrinsic XIAP IRES RNA conformation is critical for initiation complex formation and significant distortions of this conformation make it non-permissive for initiation complex formation. These data are in agreement with reports showing that structural distortions of many viral IRESes (such as HCV, FMDV, EMCV, CSFV or CrPV) render these IRESes inactive.[24,57-59] Additionally, initiation complex formation on an authentic AUG (Fig. S1B) of the RNA containing either 5′ cap (Fig. S1A) or an active IRES element (Fig. 1B) has shown that the RRL used for toeprinting assay authentically recapitulated translation machinery. These data also suggest that the structural distortion of XIAP IRES affects ribosome recruitment step and the downstream steps of initiation complex formation remain unaltered. We have previously shown that hippuristanol, an eIF4A1 and eIF4A2 specific ATPase inhibitor, does not inhibit initiation complex formation on the XIAP IRES and we hypothesized that eIF4A1 or eIF4A2 dependent ribosome scanning is thus not required to form initiation complex on XIAP IRES RNA.[15] In the present study we have expanded on this observation and show that pateamine A, an eIF4A1 and eIF4A2 allosteric inhibitor, also does not inhibit translation initiation on the XIAP IRES, but inhibits cap dependent translation initiation on GAPDH mRNA (Fig. 5C). This observation lends further support to the notion that eIF4As and ATP dependent ribosome scanning is not required for XIAP IRES translation and therefore we have decided to investigate if the ribosome is placed directly to the vicinity of AUG on XIAP IRES RNA, as it is on several viral IRESes. We have previously performed deletion analysis of the XIAP IRES and shown that XIAP IRES activity remained unaffected when a large portion (845 nt) of the 5′ UTR was deleted (to position −162 NT from

AUG) but a further deletion of 79 nucleotides (to −83 NT from AUG) resulted in 60% decrease of IRES activity.[8] In striking contrast, toeprinting analysis performed in the present study showed that deletions up to −33 NT from AUG did not inhibit initiation complex formation on XIAP IRES RNA. Therefore, we investigated if XIAP coding region (CDS) influences initiation complex formation on the XIAP IRES. Similar to pestiviral IRESes,[60] we have shown that 42 NT of XIAP coding region is involved in initiation complex formation (Fig. 3A). However, the 33 NT region of the XIAP IRES is required for the formation of translation competent initiation complex (Fig. 3B). These findings indicate that the minimal ribosome recruitment site on XIAP IRES is comprised of 33 NT of 5′ UTR and 42 NT of XIAP coding region, and the ribosome is recruited directly to the vicinity of AUG. Strikingly, our toeprinting analysis performed on the XIAP-CAT RNA chimeras showed that cap-independent translation initiation was inhibited when the 42 NT coding region of XIAP was replaced with that of CAT. However, this inhibition was relieved when a larger, 170 NT segment of the XIAP 5′ UTR was used with the 42 NT of CAT coding region (Fig. S2). These findings suggest that the full length XIAP IRES UTR in combination with CAT coding region renders the RNA conformation permissive for ribosome recruitment and therefore authenticates the use of XIAP IRES βgal-CAT bicistronic reporter construct.

For viral IRESes it has been shown that intact local structure in the vicinity of initiation codon is critical for ribosome positioning for translation initiation.[23,24,29,30,61] By performing mutational analysis in bicistroninc reporter we have shown previously that mutations in stem loop I of XIAP IRES did not alter the IRES activity.[9] However, these mutations altered only the local RNA conformation in SL-I but failed to induce RNA wide conformational changes, particularly in the vicinity of AUG. In the present study we performed additional structure-function analysis and strategic mutational analysis and show that XIAP mRNA contains an open loop conformation in the vicinity of AUG that is critical for translation initiation on the XIAP IRES (Fig. 4). Of note, a recent *in vivo* structural analysis of BACE1 mRNA has revealed that an open loop conformation of RNA in the vicinity of AUG is required for efficient translation initiation by a ribosome-shunting mechanism.[62] Furthermore, *in vivo* genome-wide structural analysis have shown that stress responsive transcripts of *Arabidopsis thaliana* seedlings contain open loop structure in front of initiation codons and this may be responsible for plasticity in their translation regulation, in particular in response to stress.[63] These data suggest that evolutionary conserved structural features exist, which promote selective translation in response to stress. Future research should be directed toward similar *in vivo* structural analysis of cellular transcripts containing IRES elements which would provide in depth information for the mechanism of cellular IRES-mediated translation regulation.

The canonical eukaryotic initiation factors are well studied for their role in cellular and viral IRES mediated translation regulation.[64,65] Extensive evidence to date suggests that eIF3 directly binds to HCV and HCV-like IRESes and aid in the formation of initiation complex,[66] and that the interaction of eIF3 with these IRESes depends on structural integrity of the IRES.[58,67] Here we show that eIF3d interacts directly with the cellular IRES (Fig. 6A). Additionally, we probed the western blot membrane with eIF3a, c and j subunits. However, due to the much lower sensitivity of antibodies against these subunits (when compared to the eIF3d antibody), we could not detect the presence of these subunits in the RNP complex formed on XIAP IRES RNA (data not shown). Importantly, eIF3 binds directly to XIAP IRES RNA, but not to the 5′ PPT mutant (Fig. 7A) which has a significantly different RNA conformation. This finding suggests that, like HCV IRES, interaction of eIF3 with XIAP IRES relies on the intrinsic structural conformation of the XIAP IRES RNA. We have further shown that 40S ribosome associated with the key initiation factors, including eIF3, was recruited onto XIAP IRES RNA, but not onto the non-functional 5′ PPT mutant (Fig. 7). Initiation complex formation on XIAP IRES RNA is poly(A) tail and PABP dependent (Fig. 5; and [15]). Additionally, eIF3 and PABP interacts cooperatively with poly(A) tailed XIAP IRES RNA (Fig. 6B) and act in synergy for ribosome recruitment on XIAP IRES RNA. Interaction between eIF3 and PABP via PAIP1 enhances ribosome recruitment by stabilizing eIF4G-PABP interaction[68-70] and we have detected significant amount of PAIP-1 in RRL (Fig. S5). Therefore, we propose that eIF3-PABP-PAIP1 interaction potentiates ribosome recruitment on the XIAP IRES RNA. Based on our findings we suggest the following mechanism of ribosome recruitment on XIAP IRES RNA (Fig. 8). The key initiation factor eIF3 (or at least some of its subunits) bind/s directly to the XIAP IRES RNA and act/s as a scaffold between RNA, ribosome and PABP. The
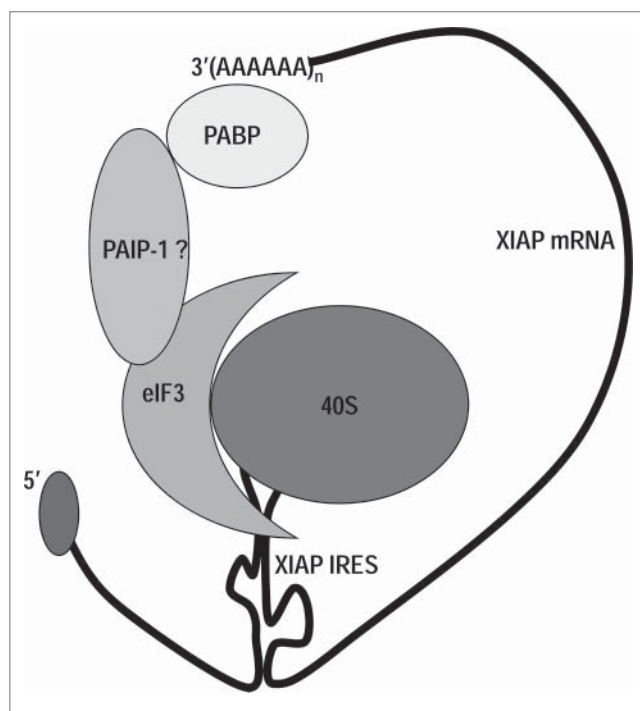

Figure 8. A proposed model illustrating mechanism of ribosome recruitment on the XIAP IRES. The scaffolding protein factor eIF3 binds directly to the XIAP IRES in an RNA conformation dependent manner. The interaction of eIF3 with PABP, likely via PAIP 1, enables RNA circularization. This RNP complex subsequently facilitates ribosome recruitment to the XIAP IRES RNA in the vicinity of AUG.

poly(A) tail bound PABP, likely via PAIP1, interacts with eIF3 to circularize XIAP mRNA. This RNP complex subsequently recruits ribosome on XIAP IRES RNA, positioning it in the vicinity of AUG in an RNA conformation-dependent manner, and allowing for subsequent 48S formation.

Materials and methods

Constructs

Previously described XIAP IRES construct,[15] which contains both streptotag-aptamer and a unique toeprint primer binding site, was used in this study. The 5′ PPT mutant, 3′ PPT mutant, PPT double mutant and SC mutants were created by site-directed mutagenesis of the XIAP IRES construct using primers listed in Table S1. GAPDH (102 NT UTR + 44 NT CDS) and XIAP non-IRES UTR (160 NT UTR + 42 NT CDS) construct were generated by replacing XIAP IRES with GAPDH or XIAP non-IRES sequences; CrPV IGR construct was generated by replacing XIAP IRES with CrPV IGR IRES (192 NT IGR IRES + 42 NT CDS; derived from plasmid pEJΔ443, a generous gift from Dr. Eric Jan). All plasmids were verified by restriction digest and sequencing.

In vitro transcription

Polymerase chain reaction (PCR) was performed to generate DNA templates for in vitro transcription of RNAs for the toeprinting assays and streptomycin affinity chromatography. Synthetic DNA oligos were obtained from IDT for GAPDH-XIAP chimera and −33 CDS mutant which were then cloned into above mentioned toeprinting plasmid. T7 promoter sequence was incorporated in the 5′ primers to allow for RNA synthesis. 51 thymine residues were added to the end of 3′ reverse primer (Table S1) to produce poly-A tailed RNA. In vitro transcription was performed using the Megashortscript kit (Ambion) to synthesize un-capped versions of RNA and mMessage mMachine kit (Ambion) was used to generate capped versions of RNA. The newly-synthesized RNA was treated with TurboDNAse (Ambion) and purified by ethanol precipitation.

Toeprinting assay

Toeprinting was performed as described[15,16] with the following modifications. Briefly, RRL (Green Hectares) was treated with RNAsein (Promega) and GMP-PNP for 5 min at 30°C. Subsequently, RNA, ATP and GTP were added as indicated, and the reactions were incubated at 30°C for further 5 min. The reaction volume was brought to 40 μl by the addition of toeprinting buffer [20 mM Tris-HCl (pH 7.6), 100 mM KOAc, 2.5 mM Mg (OAc)$_2$, 5% (wt/vol) sucrose, 2 mM DTT and 0.5 mM spermidine] and incubated at 30°C for 3 min. Subsequently, 5 pmol of toeprinting primer (5-CTCGATATGTGCATCTGTA-3; 5′ end-labeled with IRDye^{TM}800) was added and reaction was incubated on ice for 10 min. 1 mM dNTPs, 5 mM Mg(OAc)$_2$ and 1 μl of avian myeloblastosis virus reverse transcriptase (Promega) were added to the reaction and the final volume was brought to 50 μl by toeprinting buffer. Primer extension was

allowed to occur for 45 min at 30°C. The cDNA products were purified by phenol:chloroform extraction and analyzed on a standard 6% sequencing gel using a model 4200 IR2 sequence analyzer (LI-COR, Lincoln, Nebraska, USA). The concentrations of the toeprinting assay components are as follows unless otherwise specified: RRL; 5 or 15 μl (as indicated) GMP-PNP; 1.7 mM, ATP; 1.82 mM, GTP; 1.8 mM, RNA; 800 ng.

RNA-Streptomycin affinity chromatography

S10 cytoplasmic lysate from HeLa cells was prepared as described.[17] Briefly, HeLa-S cells (2 ml packed cell volume (PCV); Biovest International, Tampa, FL, USA) were resuspended in 2 ml of hypotonic buffer [10 mM Tris-HCl (pH 7.6), 1.5 mM MgCl2, 10 mM KCl, 0.5 mM DTT] containing EDTA-free protease inhibitor cocktail (Roche) and lysed using dounce homogenizer (30 strokes, pestle B). A mixture of 4 ml of HeLa S10 cytoplasmic lysate and 12 ml binding buffer [20 mM Tris (pH 7.6), 10 mM MgCl$_2$, 120 mM KCl, 8% sucrose, 2 mM DTT] containing EDTA-free protease inhibitor cocktail (Roche) and ribonuclease inhibitor (Promega) was incubated at 37°C for 10 min. An in vitro transcribed, strepto-tagged XIAP IRES RNA or strepto-tagged GAPDH RNA was added to the mixture and further incubated for 10 min at 37°C. RNA-dihydrostreptomycin affinity chromatography was performed as described[15,18] and the RNA associated proteins were analyzed using protein gel blot analysis.

Western blot analysis

Proteins in equal volumes of affinity chromatography effluents or proteins associated with 700 nM 40S ribosome were resolved by 10% sodium dodecyl sulfate polyacrylamide gel electrophoresis (SDS-PAGE), transferred to nitrocellulose membranes and probed with antibodies against eIF3d (Abcam, Ab155419), eIF4E (Cell Signaling, #9742), eIF4A (Cell Signaling, #2013), eIF2α (Cell Signaling, #9722), eIF4GI (Cell Signaling, #2858), PABP (Abcam, Ab21060), eIF1A (Abcam, Ab177939), PAIP-1 (Abcam, Ab175211) or ribosomal protein S6 (Cell Signaling, #2317). Membranes were then incubated with species-specific horseradish peroxidase-conjugated secondary antibody (Cell Signaling) followed by detection with ECL substrate (Pierce).

RNA structure determination

In vitro transcribed RNA was probed with 130 mM N-methylisatoic anhydride (NMIA) following the protocol of Wilkinson et al.[19] with the modifications published by Baird et al.[9] NMIA reactive sites were used as constraints in RNASTRUCTURE[20] to predict the secondary structure of RNA.

Protein purification

GST tagged PAIP2 protein was purified as described.[21] Pgex-6P-Paip2 (GST-PAIP2; a generous gift from Dr. Nahum Sonenberg) was transformed in Escherichia coli BL21 competent cells and the production of GST-PAIP2 was induced by addition of 0.5 mM IPTG into the culture broth during mid-logarithmic growth phase. GST-PAIP2 expressing cells

were harvested by centrifugation and lysed by ultra-sonication in presence of EDTA-free protease inhibitor cocktail (Roche). GST-PAIP2 protein was captured on GSTrap^{TM} column (GE life sciences) and eluted with step-gradient of reduced glutathione. Effluent fractions were subjected to SDS-PAGE analysis followed by Comassie brilliant blue staining. Homogeneous effluent fraction was dialyzed against binding buffer (20 mM Tris-HCl, pH 7.4, 200 mM KCl, 1% (vol/vol) glycerol and 1 mM DTT) and concentrated using AmiconUltra^{TM} (Millipore). eIF3 was purified and described previously.[22]

Purification of 40S ribosome subunits

S10 cytoplasmic lysate from HeLa cells was prepared as described above. S10 lysate was treated with 1 mM puromycin and 25 mM EDTA first for 10 min on ice followed by 10 min incubation at 30°C. We avoided 0.5M KCl treatment which may strip-off ribosome associated proteins. Ribosomal subunits were separated on 15-40% sucrose gradients (20 mM Tris-HCl, pH 7.4, 100 mM KOAc, 200 mM KCl, 2.5 mM MgCl$_2$ and 2 mM DTT) as described.[23,24] Ribosomal subunit peaks were monitored by measuring absorbance at 260 nm. Buffer of the isolated 40S was exchanged to toeprinting buffer using AmiconUltra^{TM} (Millipore). The concentration of 40S ribosomal subunit was determined by UV spectrophotometry using the conversion 1 A$_{260}$ = 50 nM 40S ribosome. Association of eIFs with purified 40S was verified by western blot analysis.

Non-denaturing gel mobility shift assay

Non-denaturing gel mobility shift assay for eIF3-RNA complex and 40S-RNA complex was performed as described[23,24] with a few modifications. Briefly, radiolabeled RNA (10K cpm) was incubated with either 14 nM 40S ribosome or 0.1 μg and 0.2 μg human eIF3 complex for 15 min at 37°C. Non-denaturing agarose gel electrophoresis was performed as described.[16] Agarose gel was fixed in 30% (vol/vol) methanol and 10% (vol/vol) acetic acid solution for 30 min. Subsequently, the gel was dried on a gel dryer first with vacuum only for 45 min followed by 55°C and 80°C for 45 min each. Mobility shifts were determined by exposing dried gel to X-ray films.

Disclosure of potential conflicts of interest

No potential conflicts of interest were disclosed.

References

1. Spriggs KA, Stoneley M, Bushell M, Willis AE. Re-programming of translation following cell stress allows IRES-mediated translation to predominate. Biol Cell 2008; 100:27-38; PMID:18072942; http://dx.doi.org/10.1042/BC20070098
2. Spriggs KA, Bushell M, Willis AE. Translational regulation of gene expression during conditions of cell stress. Mol Cell 2010; 40:228-37; PMID:20965418; http://dx.doi.org/10.1016/j.molcel.2010.09.028
3. Holcik M, Sonenberg N. Translational control in stress and apoptosis. Nat Rev Mol Cell Biol 2005; 6:318-27; PMID:15803138; http://dx.doi.org/10.1038/nrm1618
4. Silvera D, Formenti SC, Schneider RJ. Translational control in cancer. Nat Rev Cancer 2010; 10:254-66; PMID:20332778; http://dx.doi.org/10.1038/nrc2824
5. Ruggero D. Translational control in cancer etiology. Cold Spring Harb Perspect Biol 2013; 1:5-2. pii: a012336; PMID: 22767671; http://dx.doi/ 0.1101/cshperspect.a012336.
6. Pelletier J, Sonenberg N. Internal initiation of translation of eukaryotic mRNA directed by a sequence derived from poliovirus RNA. Nature 1988; 334:320-5; PMID:2839775; http://dx.doi.org/10.1038/334320a0
7. Jackson RJ. The current status of vertebrate cellular mRNA IRESs. Cold Spring Harb Perspect Biol. 2013; 1:5-2; PMID:23378589; http://dx.doi/10.1101/cshperspect.a011569.
8. Holcik M, Lefebvre C, Yeh C, Chow T, Korneluk RG. A new internal-ribosome-entry-site motif potentiates XIAP-mediated cytoprotection. Nat Cell Biol 1999; 1:190-2; PMID:10559907; http://dx.doi.org/10.1038/11109
9. Baird SD, Lewis SM, Turcotte M, Holcik M. A search for structurally similar cellular internal ribosome entry sites. Nucleic Acids Res 2007; 35:4664-77; PMID:17591613; http://dx.doi.org/10.1093/nar/gkm483
10. Liwak U, Thakor N, Jordan LE, Roy R, Lewis SM, Pardo OE, Seckl M, Holcik M. Tumor suppressor PDCD4 represses internal ribosome entry site-mediated translation of antiapoptotic proteins and is regulated by S6 kinase 2. Mol Cell Biol 2012; 32:1818-29; PMID:22431522; http://dx.doi.org/10.1128/MCB.06317-11
11. Holcik M, Korneluk RG. Functional characterization of the X-linked inhibitor of apoptosis (XIAP) internal ribosome entry site element: role of La autoantigen in XIAP translation. Mol Cell Biol 2000; 20:4648-57; PMID:10848591; http://dx.doi.org/10.1128/MCB.20.13.4648-4657.2000
12. Holcik M, Gordon BW, Korneluk RG. The internal ribosome entry site-mediated translation of antiapoptotic protein XIAP is modulated by the heterogeneous nuclear ribonucleoproteins C1 and C2. Mol Cell Biol 2003; 23:280-8; PMID:12482981; http://dx.doi.org/10.1128/MCB.23.1.280-288.2003
13. Lewis SM, Veyrier A, Hosszu Ungureanu N, Bonnal S, Vagner S, Holcik M. Subcellular relocalization of a trans-acting factor regulates XIAP IRES-dependent translation. Mol Biol Cell 2007; 18:1302-11; PMID:17287399; http://dx.doi.org/10.1091/mbc.E06-06-0515
14. Hundsdoerfer P, Thoma C, Hentze MW Eukaryotic translation initiation factor 4GI and p97 promote cellular internal ribosome entry sequence-driven translation. Proc Natl Acad Sci U S A 2005; 102:13421-6; Epub 12005 Sep 13427; PMID:16174738; http://dx.doi.org/10.1073/pnas.0506536102
15. Thakor N, Holcik M. IRES-mediated translation of cellular messenger RNA operates in eIF2alpha- independent manner during stress. Nucleic Acids Res 2012; 40:541-52; PMID:21917851; http://dx.doi.org/10.1093/nar/gkr701
16. Locker N, Lukavsky PJ. A practical approach to isolate 48S complexes: affinity purification and analyses. Methods Enzymol 2007; 429:83-

104; PMID:17913620; http://dx.doi.org/10.1016/S0076-6879(07)29005-6

17. Graber TE, Baird SD, Kao PN, Mathews MB, Holcik M. NF45 functions as an IRES trans-acting factor that is required for translation of cIAP1 during the unfolded protein response. Cell Death Differ 2010; 17:719-29; PMID:19893574; http://dx.doi.org/10.1038/cdd.2009.164

18. Faye MD, Graber TE, Liu P, Thakor N, Baird SD, Durie D, Holcik M. Nucleotide composition of cellular internal ribosome entry sites defines dependence on NF45 and predicts a posttranscriptional mitotic regulon. Mol Cell Biol 2013; 33:307-18; PMID:23129811; http://dx.doi.org/10.1128/MCB.00546-12

19. Wilkinson KA, Merino EJ, Weeks KM. Selective 2′-hydroxyl acylation analyzed by primer extension (SHAPE): quantitative RNA structure analysis at single nucleotide resolution. Nat Protoc 2006; 1:1610-6; PMID:17406453; http://dx.doi.org/10.1038/nprot.2006.249

20. Mathews DH, Disney MD, Childs JL, Schroeder SJ, Zuker M, Turner DH. Incorporating chemical modification constraints into a dynamic programming algorithm for prediction of RNA secondary structure. Proc Natl Acad Sci U S A 2004; 101:7287-92; Epub 2004 May 7283; PMID:15123812; http://dx.doi.org/10.1073/pnas.0401799101

21. Svitkin YV, Sonenberg N. An efficient system for cap- and poly(A)-dependent translation in vitro. Methods Mol Biol 2004; 257:155-70; PMID:14770004

22. Sun C, Todorovic A, Querol-Audi J, Bai Y, Villa N, Snyder M, Ashchyan J, Lewis CS, Hartland A, Gradia S, et al. Functional reconstitution of human eukaryotic translation initiation factor 3 (eIF3). Proc Natl Acad Sci U S A 2011; 108:20473-8; Epub 1116822011 Dec 1116821101; PMID:22135459; http://dx.doi.org/10.1073/pnas.1116821108

23. Jan E, Sarnow P. Factorless ribosome assembly on the internal ribosome entry site of cricket paralysis virus. J Mol Biol 2002; 324:889-902; PMID:12470947; http://dx.doi.org/10.1016/S0022-2836(02)01099-9

24. Jang CJ, Lo MC, Jan E. Conserved element of the dicistrovirus IGR IRES that mimics an E-site tRNA/ribosome interaction mediates multiple functions. J Mol Biol 2009; 387:42-58; Epub 2009 Jan 1029; PMID:19361441; http://dx.doi.org/10.1016/j.jmb.2009.01.042

25. Riley A, Jordan LE, Holcik M. Distinct 5′ UTRs regulate XIAP expression under normal growth conditions and during cellular stress. Nucleic Acids Res 2010; 38:4665-74; PMID:20385593; http://dx.doi.org/10.1093/nar/gkq241

26. Shirokikh NE, Alkalaeva EZ, Vassilenko KS, Afonina ZA, Alekhina OM, Kisselev LL, Spirin AS. Quantitative analysis of ribosome-mRNA complexes at different translation stages. Nucleic Acids Res 2010; 38: e15; Epub 2009 Nov 1012; PMID:19910372; http://dx.doi.org/10.1093/nar/gkp1025

27. Holcik M, Graber T, Lewis SM, Lefebvre CA, Lacasse E, Baird S. Spurious splicing within the XIAP 5′ UTR occurs in the Rluc/Fluc but not the {beta}gal/CAT bicistronic reporter system. RNA 2005; 11:1605-9; PMID:16177136; http://dx.doi.org/10.1261/rna.2158605

28. Hellen CU, Sarnow P. Internal ribosome entry sites in eukaryotic mRNA molecules. Genes Dev 2001; 15:1593-612; PMID:11445534; http://dx.doi.org/10.1101/gad.891101

29. Berry KE, Waghray S, Mortimer SA, Bai Y, Doudna JA. Crystal structure of the HCV IRES central domain reveals strategy for start-codon positioning. Structure 2011; 19:1456-66; PMID:22000514; http://dx.doi.org/10.1016/j.str.2011.08.002

30. Berry KE, Waghray S, Doudna JA. The HCV IRES pseudoknot positions the initiation codon on the 40S ribosomal subunit. RNA 2010; 16:1559-69; Epub 2192010 Jun 2197228; PMID:20584896; http://dx.doi.org/10.1261/rna.2197210

31. Thoma C, Bergamini G, Galy B, Hundsdoerfer P, Hentze MW. Enhancement of IRES-mediated translation of the c-myc and BiP mRNAs by the Poly(A) tail is independent of intact eIF4G and PABP. Mol Cell 2004; 15:925-35; PMID:15383282; http://dx.doi.org/10.1016/j.molcel.2004.08.021

32. Pestova TV, Lorsch JR, Hellen CU. In Mathews, M. B., Sonenberg, N. and Hershey, J. W. B. (eds.), Translational Control in Biology and Medicine. Cold Spring Harbor, New York: Cold Spring Harbor Laboratory Press 2007; pp. 87-128.

33. Lewis SM, Cerquozzi S, Graber TE, Ungureanu NH, Andrews M, Holcik M. The eIF4G homolog DAP5/p97 supports the translation of select mRNAs during endoplasmic reticulum stress. Nucleic Acids Res 2008; 36:168-78; PMID:18003655; http://dx.doi.org/10.1093/nar/gkm1007

34. Lopez de Quinto S, Martinez-Salas E. Interaction of the eIF4G initiation factor with the aphthovirus IRES is essential for internal translation initiation in vivo. RNA 2000; 6:1380-92; PMID:11073214; http://dx.doi.org/10.1017/S1355838200000753

35. Silvera D, Arju R, Darvishian F, Levine PH, Zolfaghari L, Goldberg J, Hochman T, Formenti SC, Schneider RJ. Essential role for eIF4GI overexpression in the pathogenesis of inflammatory breast cancer. Nat Cell Biol 2009; 11:903-8; PMID:19525934; http://dx.doi.org/10.1038/ncb1900

36. Braunstein S, Karpisheva K, Pola C, Goldberg J, Hochman T, Yee H, Cangiarella J, Arju R, Formenti SC, Schneider RJ. A hypoxia-controlled cap-dependent to cap-independent translation switch in breast cancer. Mol Cell 2007; 28:501-12; PMID:17996713; http://dx.doi.org/10.1016/j.molcel.2007.10.019

37. Svitkin YV, Evdokimova VM, Brasey A, Pestova TV, Fantus D, Yanagiya A, Imataka H, Skabkin MA, Ovchinnikov LP, Merrick WC, et al. General RNA-binding proteins have a function in poly(A)-binding protein-dependent translation. EMBO J 2009; 28:58-68; Epub 2008 Dec 1011; PMID:19078965; http://dx.doi.org/10.1038/emboj.2008.259

38. Holcik M, Korneluk RG. XIAP, the guardian angel. Nat Rev Mol Cell Biol 2001; 2:550-6; PMID:11433370; http://dx.doi.org/10.1038/35080103

39. Holcik M, Yeh C, Korneluk RG, Chow T. Translational upregulation of X-linked inhibitor of apoptosis (XIAP) increases resistance to radiation induced cell death. Oncogene 2000; 19:4174-7; PMID:10962579; http://dx.doi.org/10.1038/sj.onc.1203765

40. Durie D, Lewis SM, Liwak U, Kisilewicz M, Gorospe M, Holcik M. RNA-binding protein HuR mediates cytoprotection through stimulation of XIAP translation. Oncogene 2011; 30:1460-9; PMID:21102524; http://dx.doi.org/10.1038/onc.2010.527

41. Bevilacqua E, Wang X, Majumder M, Gaccioli F, Yuan CL, Wang C, Zhu X, Jordan LE, Scheuner D, Kaufman RJ, et al. eIF2alpha phosphorylation tips the balance to apoptosis during osmotic stress. J Biol Chem 2010; 285:17098-111; PMID:20338999; http://dx.doi.org/10.1074/jbc.M110.109439

42. Yoon A, Peng G, Brandenburg Y, Zollo O, Xu W, Rego E, Ruggero D. Impaired control of IRES-mediated translation in X-linked dyskeratosis congenita. Science 2006; 312:902-6; PMID:16690864; http://dx.doi.org/10.1126/science.1123835

43. Gu L, Zhu N, Zhang H, Durden DL, Feng Y, Zhou M. Regulation of XIAP translation and induction by MDM2 following irradiation. Cancer Cell 2009; 15:363-75; PMID:19411066; http://dx.doi.org/10.1016/j.ccr.2009.03.002

44. Filbin ME, Kieft JS Toward a structural understanding of IRES RNA function. Curr Opin Struct Biol 2009; 19:267-76; Epub 2009 Apr 1019; PMID:19362464; http://dx.doi.org/10.1016/j.sbi.2009.03.005

45. Kieft JS, Zhou K, Jubin R, Murray MG, Lau JY, Doudna JA. The hepatitis C virus internal ribosome entry site adopts an ion-dependent tertiary fold. J Mol Biol 1999; 292:513-29; PMID:10497018; http://dx.doi.org/10.1006/jmbi.1999.3095

46. Odreman-Macchioli F, Baralle FE, Buratti E. Mutational analysis of the different bulge regions of the HCV domain II and their influence on IRES translational ability. J Biol Chem 2001; 276:41648-55; PMID:11498532; http://dx.doi.org/10.1074/jbc.M104128200

47. Brown EA, Day SP, Jansen RW, Lemon SM. The 5′ nontranslated region of hepatitis A virus RNA: secondary structure and elements required for translation in vitro. J Virol 1991; 65:5828-38; PMID:1656072

48. Kolupaeva VG, Hellen CU, Shatsky IN. Structural analysis of the interaction of the pyrimidine tract-binding protein with the internal ribosomal entry site of encephalomyocarditis virus and foot-and-mouth disease virus RNAs. RNA 1996; 2:1199-212; PMID:8972770

49. Hoffman MA, Palmenberg AC. Mutational analysis of the J-K stem-loop region of the encephalomyocarditis virus IRES. J Virol 1995; 69:4399-406; PMID:7769702

50. Yaman I, Fernandez J, Liu H, Caprara M, Komar AA, Koromilas AE, Zhou L, Snider MD, Scheuner D, Kaufman RJ, et al. The zipper model of translational control. A small upstream ORF is the switch that controls structural remodeling of an mRNA leader. Cell 2003; 113:519-31; PMID:12757712; http://dx.doi.org/10.1016/S0092-8674(03)00345-3

51. Mitchell SA, Spriggs KA, Coldwell MJ, Jackson RJ, Willis AE. The Apaf-1 internal ribosome entry segment attains the correct structural conformation for function via interactions with PTB and unr. Mol Cell 2003; 11:757-71; PMID:12667457; http://dx.doi.org/10.1016/S1097-2765(03)00093-5

52. Jopling CL, Spriggs KA, Mitchell SA, Stoneley M, Willis AE. L-Myc protein synthesis is initiated by internal ribosome entry. RNA 2004; 10:287-98; PMID:14730027; http://dx.doi.org/10.1261/rna.5138804

53. Bonnal S, Schaeffer C, Creancier L, Clamens S, Moine H, Prats AC, Vagner S. A single internal ribosome entry site containing a G quartet RNA structure drives fibroblast growth factor 2 gene expression at four alternative translation initiation codons. J Biol Chem 2003; 278:39330-6; Epub 32003 Jul 39311; PMID:12857733; http://dx.doi.org/10.1074/jbc.M305580200

54. Martineau Y, Le Bec C, Monbrun L, Allo V, Chiu IM, Danos O, Moine H, Prats H, Prats AC. Internal ribosome entry site structural motifs conserved among mammalian fibroblast growth factor 1 alternatively spliced mRNAs. Mol Cell Biol 2004; 24:7622-35; PMID:15314170; http://dx.doi.org/10.1128/MCB.24.17.7622-7635.2004

55. Le Quesne JP, Stoneley M, Fraser GA, Willis AE. Derivation of a structural model for the c-myc IRES. J Mol Biol 2001; 310:111-26; PMID:11419940; http://dx.doi.org/10.1006/jmbi.2001.4745

56. Pickering BM, Mitchell SA, Spriggs KA, Stoneley M, Willis AE. Bag-1 internal ribosome entry segment activity is promoted by structural changes mediated by Poly(rC) binding protein 1 and recruitment of polypyrimidine tract binding protein 1. Mol Cell Biol 2004; 24:5595-605; PMID:15169918; http://dx.doi.org/10.1128/MCB.24.12.5595-5605.2004

57. Willcocks MM, Locker N, Gomwalk Z, Royall E, Bakhshesh M, Belsham GJ, Idamakanti N, Burroughs KD, Reddy PS, Hallenbeck PL. et al. Structural features of the Seneca Valley virus internal ribosome entry site (IRES) element: a picornavirus with a pestivirus-like IRES. J Virol 2011; 85:4452-61; Epub 02011 Feb 01116; PMID:21325406; http://dx.doi.org/10.1128/JVI.01107-10

58. Sizova DV, Kolupaeva VG, Pestova TV, Shatsky IN, Hellen CU. Specific interaction of eukaryotic translation initiation factor 3 with the 5′ nontranslated regions of hepatitis C virus and classical swine fever virus RNAs. J Virol 1998; 72:4775-82; PMID:9573242

59. Balvay L, Soto Rifo R, Ricci EP, Decimo D, Ohlmann T. Structural and functional diversity of viral IRESes. Biochim Biophys Acta 2009; 1789:542-57; Epub 2009 Jul 1024; PMID:19632368; http://dx.doi.org/10.1016/j.bbagrm.2009.07.005

60. Fletcher SP, Ali IK, Kaminski A, Digard P, Jackson RJ. The influence of viral coding sequences on pestivirus IRES activity reveals further parallels with translation initiation in prokaryotes. RNA 2002; 8:1558-71; PMID:12515388 http://dx.doi.org/10.1017/S135583820202303

61. Jubin R, Vantuno NE, Kieft JS, Murray MG, Doudna JA, Lau JY, Baroudy BM. Hepatitis C virus internal ribosome entry site (IRES) stem loop IIId contains a phylogenetically conserved GGG triplet essential for translation and IRES folding. J Virol 2000; 74:10430-7; PMID:11044087; http://dx.doi.org/10.1128/JVI.74.22.10430-10437.2000

62. Koh DC, Edelman GM, Mauro VP. Physical evidence supporting a ribosomal shunting mechanism of translation initiation for BACE1 mRNA. Translation 2013; 1, e24400; http://dx.doi.org/10.4161/trla.24400

63. Ding Y, Tang Y, Kwok CK, Zhang Y, Bevilacqua PC, Assmann SM. In vivo genome-wide profiling of RNA secondary structure reveals novel regulatory features. Nature 2014; 505:696-700; Epub 12013 Nov 12724; PMID:24270811; http://dx.doi.org/10.1038/nature12756

64. Komar AA, Mazumder B, Merrick WC. A new framework for understanding IRES-mediated translation. Gene 2012; 502:75-86; PMID:22555019; http://dx.doi.org/10.1016/j.gene.2012.04.039

65. Komar AA, Hatzoglou M. Cellular IRES-mediated translation: the war of ITAFs in pathophysiological states. Cell Cycle 2011; 10:229-40; PMID:21220943; http://dx.doi.org/10.4161/cc.10.2.14472

66. Hashem Y, des Georges A, Dhote V, Langlois R, Liao HY, Grassucci RA, Pestova TV, Hellen CU, Frank J. Hepatitis-C-virus-like internal ribosome entry sites displace eIF3 to gain access to the 40S subunit. Nature 2013; 503:539-43; Epub 12013 Nov 12653; PMID:24185006; http://dx.doi.org/10.1038/nature12658

67. Collier AJ, Gallego J, Klinck R, Cole PT, Harris SJ, Harrison GP, Aboul-Ela F, Varani G, Walker S. A conserved RNA structure within the HCV IRES eIF3-binding site. Nat Struct Biol 2002; 9:375-80; PMID:11927954

68. Derry MC, Yanagiya A, Martineau Y, Sonenberg N. Regulation of poly (A)-binding protein through PABP-interacting proteins. Cold Spring Harb Symp Quant Biol 2006; 71:537-43; PMID:17381337; http://dx.doi.org/10.1101/sqb.2006.71.061

69. Martineau Y, Derry MC, Wang X, Yanagiya A, Berlanga JJ, Shyu AB, Imataka H, Gehring K, Sonenberg N. Poly(A)-binding protein-interacting protein 1 binds to eukaryotic translation initiation factor 3 to stimulate translation. Mol Cell Biol 2008; 28:6658-67; Epub 02008 Aug 00725; PMID:18725400; http://dx.doi.org/10.1128/MCB.00738-08

70. Martineau Y, Wang X, Alain T, Petroulakis E, Shahbazian D, Fabre B, Bousquet-Dubouch MP, Monsarrat B, Pyronnet S, Sonenberg N. Control of Paip1-eukayrotic translation initiation factor 3 interaction by amino acids through S6 kinase. Mol Cell Biol 2014; 34:1046-53; Epub 02014 Jan 01076; PMID:24396066; http://dx.doi.org/10.1128/MCB.01079-13